energies

MDPI

Article

Sewage Sludge Valorization via Hydrothermal Carbonization: Optimizing Dewaterability and Phosphorus Release

Taina Lühmann and Benjamin Wirth *

Biorefineries Department, Deutsches Biomasseforschungszentrum Gemeinnützige GmbH, Torgauer Straße 116, 04347 Leipzig, Germany; taina.luehmann@ru.nl

* Correspondence: benjamin.wirth@dbfz.de; Tel.: +49-341-2434-449

Received: 25 July 2020; Accepted: 26 August 2020; Published: 26 August 2020



Abstract: As the use of sewage sludge as a fertilizer in agriculture is increasingly restricted in the European Union, other ways to utilize this waste stream need to be developed. Sewage sludge is an ideal input material for the process of hydrothermal carbonization, as it can convert wet biomass into a solid energy carrier with increased mechanical dewaterability. Digested sewage sludge was hydrothermally carbonized at 160–200 °C for 30–60 min with initial pH levels of 1.93–8.08 to determine optimal reaction conditions for enhanced dewaterability and phosphorus release into the liquid phase. Design of experiments was used to develop response surface models, which can be applied to optimize the process conditions. For optimal dewaterability and phosphorus release, low initial pH values (pH 1.93) and mild temperatures around 170 °C are favorable. Because holding time had no statistically relevant effect, a dependency of reaction time was investigated. Though it did not yield substantially different results, it could be included in investigations of short reaction times prospectively. Low reaction temperatures and short holding times are desirable considering economic reasons for scale-up, while the high acid consumption necessary to achieve these results is unfavorable.

Keywords: dry matter; moisture; dewatering; sewage sludge; hydrothermal treatment; phosphorus; RSM; DoE; optimization; regression model

1. Introduction

Sewage sludge is widely used in agriculture because high contents of phosphorus, nitrogen, and potassium, as well as organic carbon make it a favorable organic fertilizer [1,2]. Because of concerning substances, such as heavy metals, organic residues, microplastics, and various pathogens, stronger regulations regarding the use as fertilizer have been passed. This has been combined with a requirement to recover phosphorus from sewage sludge in countries such as Germany [3,4], so that new ways for valorization are sought after. After landfilling became restricted in the European Union (EU) in 1999, incineration has become the preferred solution in the EU-15 countries [5]. During incineration, sewage sludge can be mono-combusted in specifically designed furnaces, co-combusted in existing waste incineration plants or added in small quantities in cement kilns [6]. Thermal dewatering, an energy intensive process, is the major drawback of incineration [6].

Hydrothermal carbonization (HTC) is a process that can convert sewage sludge into a more easily mechanically dewaterable substance by breaking up the cell structure, thereby releasing bound water [7–10]. Essentially, it is a process that converts biomass in hot pressurized water yielding an upgraded solid biofuel [11,12]. Typical reaction conditions reported in literature are 180 to 250 °C for 1 to 12 h holding time [11] at an elevated pressure due to water saturation pressure and additional

pressure by gaseous compounds formed during the reaction. To measure the dewaterability of sewage sludge, different approaches such as filtration and mechanical dewatering were examined. Danso-Boateng et al. [8] used a filtration cell and calculated the specific cake resistance as a measure for dewaterability. They found that the reaction temperature was the defining factor for dewaterability, especially when compared to holding time. When Escala et al. [9] mechanically dewatered hydrochar (HC) from stabilized sewage sludge that was acidified, they were able to reach dry matter contents of 52 ± 5.5%, compared to the dry matter content of sewage sludge of 30%. Besides improved dewaterability, another advantage of applying HTC to sewage sludge is the opportunity for phosphorus recovery, the most valuable component of wastewater. Distribution of phosphorus in liquid and solid phase as well as chemical composition has been increasingly studied [13–16]. Shi et al. [14] investigated the effect of initial pH and reaction temperature on the distribution of phosphorus. They found that higher temperatures caused phosphorus to be more present in the solid phase while adding large amounts of acid could shift phosphorus into the liquid phase.

The aim of this study is to investigate the dewaterability and phosphorus release of hydrothermally treated sewage sludge as minimum required reaction conditions are yet to be determined. A method to investigate the optimal reaction conditions in a defined reaction space is facilitated by a Design of Experiments (DoE)/Response Surface Model (RSM) approach. For HTC, this has been already utilized frequently [13,17–20] and for sewage sludge dewatering after HTC by Danso-Boateng et al. [8]. While they tested the filterability as an indicator for dewatering, the objective of this study was to take a more practical approach by investigating mechanical dewatering using a screw press at lab-scale. This experimental set-up was implemented to reflect a possible industrial application. Sewage sludge was used as received (without any pre-treatment) from a wastewater treatment plant (WWTP) to identify if mild HTC conditions are suitable for valorization.

Although the process parameters reaction temperature, holding time and initial pH all play a role on phosphorus release and dewaterability, they have only been investigated individually so far. To also consider interaction effects, a DoE approach was taken. This allowed for the development of regression models to predict the above-mentioned parameters as well as typical HTC characteristics. Reaction conditions that are close to industrial applicability, for which low reaction temperatures and short holding times are of interest, were investigated.

2. Materials and Methods

2.1. Digested Sewage Sludge

Digested sewage sludge (DSS) was collected from a municipal WWTP in Leipzig, Germany, where the wastewater undergoes mechanical (screening, grit removal, primary sedimentation), chemical (phosphate precipitation) and biological treatment (aeration reactor, secondary sedimentation). Sludge stabilization includes sludge thickening, digestion, and mechanical dewatering, reaching a dry matter content of 24.3%. The composition of the sample used in this study can be found in Table 1. A sample of approximately 30 L was homogenized and separated into 27 subsamples, which were stored at 4 °C. Before being used in the experiments, they were left to warm up at room temperature.

Table 1. Properties of the tested samples with standard deviations given in parentheses.

C ‡	H ‡	N ‡	S ‡	O ‡	Ash †	HHV_{meas} †	HHV_{calc}
($\%_{db}$)						(MJ kg_{db}^{-1})	
32.5 (±0.24)	4.7 (±0.05)	5 (±0.04)	1.7 (±0.01)	15.2 (±0.33)	40.9 (±0.11)	14.3 (±0.10)	13.4

‡ = triplicates; † = duplicates; HHV = higher heating value; meas = measured; calc = calculated; db = dry basis.

The calculated higher heating value (HHV) is slightly lower than the actual measured one as high ash contents of a sample can severely impact the results of various calculation formulas [21]. However, the correlation of ultimate analysis data and HHV used here is reported to fit measured HHVs of HCs very well and the value for DSS was added as a comparison.

2.2. Experimental Method

The DoE included the variation of reaction temperature, holding time, and initial pH. A face-centered central composite design (FCCD) was chosen. Corner points were carried out in duplicate and the center point in triplicate, resulting in 27 experiments. The reaction conditions were (i) reaction temperature: 160, 180, 200 °C, (ii) holding time (starting when the reaction temperature was reached): 30, 60, 90 min, and (iii) initial pH: 2, 4.5, 7. Though holding time only accounts for part of the timespan during which reactions take place, it is the common measure for comparison of HTC studies. For sewage sludge, Escala et al. [9] used the timespan above 180 °C for each experiment. Wang et al. [22] concluded that the conversion of sewage sludge starts at around 130–150 °C, observed by a rapid rise of the organic load found in process water. However, they did not observe decomposition of these organic compounds below 180 °C. In this study, it was investigated if using the timespan above 140 °C instead of holding time for analysis would yield substantially different regression models, in accordance to the values provided by Wang et al. [7].

A graphical illustration of the design space can be found in Figure 1 and the randomized experimental design in Table A1 in Appendix A.

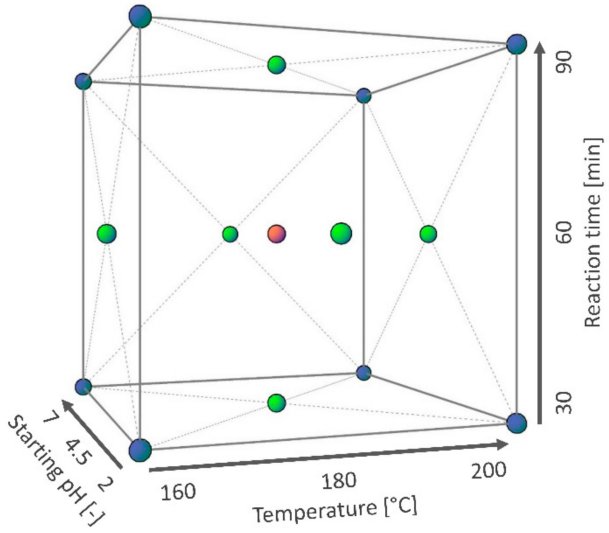


Figure 1. Design space of the face-centered central composite design (FCCD), red dots indicate triplicates, green dots duplicates, and blue dots single repetitions.

In preparation for the pH adjustment, the amount of acid needed for the targeted pH levels was determined according to DIN EN 15933 [23]. After homogenizing a mixture of 10 g of sludge and 100 mL of deionized water on a vibrating plate for 10 min at 130 rpm, concentrated sulfuric acid (18 M) was added whilst stirring until the desired pH levels were reached and held constant for 30 min. The amount of acid needed for the actual amount of sludge could then be extrapolated from these results.

For each experiment, around 350 g of DSS were weighed out and the calculated amount of sulfuric acid (18 M) was added. Of that mixture, 290 g were used for the HTC experiment and 10 g for pH measurement of the acidified sample. The measured pH was later used for regression modeling instead of the targeted pH. Except for the addition of acid, the DSS was not further diluted with water but utilized as received from the WWTP. The experiments were conducted in a 500 mL high-pressure

stirred-tank reactor made of stainless steel (BR-500, Berghof Products + Instruments GmbH, Eningen unter Achalm, Germany). The stirrer was set to 100 rpm and the reactor was heated up electrically with a heating rate of 2 K min^{-1}. After reaching the desired temperature, the reactor temperature was kept constant over the holding time. Then, the heater of the reactor was switched off and the reactor was allowed to cool down to room temperature by the environment.

After the process, the HC-water-slurry was separated with a screw press with an integrated scale. The screw press was tightened until a pressure of 300 kg (which corresponds to 2.2 bar) was applied and retightened when the weight dropped by 10 kg. Pressing was stopped when there was no liquid flow for more than one minute. After the pressing process was completed, the HC was divided into two homogeneous samples according to DIN EN ISO 14780 [24] by coning and quartering. The HC was dried and the process water was stored at 4 °C until further use.

2.3. Analytics

In all solid samples (DSS and HC), dry matter content, elemental composition (C, H, N, S) and ash content was analyzed. Additionally, HHV of DSS was measured and the concentrations of phosphorus analyzed in DSS as well as process water.

Dry matter content was determined by placing the samples in a drying oven at 105 °C overnight referring to DIN EN ISO 18134-3 [25]. Elemental carbon, hydrogen, nitrogen, and sulfur (C, H, N, S) were measured according to DIN EN 15104 [26] with an elemental analyzer (vario MACRO CUBE, Elementar Analysensysteme GmbH, Langenselbold, Germany). Ash content was determined by incineration at 550 °C according to DIN EN 14775 [27] and the oxygen content was calculated by difference. HHV was determined by combustion with oxygen in a bomb calorimeter (Parr Instrument GmbH, Moline, IL, USA), according to DIN EN ISO 18125 [28]. Phosphorus was determined according to DIN EN ISO 11885 [29] with a spectrometer (ICP-OES Icap 6300, Thermo Fisher Scientific, Waltham, MA, USA). Every sample was analyzed three times.

2.4. Calculations

Solid yields based on dry matter (DM) were calculated according to Equation (1) with respect to the mass of DSS put into the reactor and the mass of HC after the reaction:

$$\text{Solid yield } (\%_{db}) = \frac{m_{char} \times DM_{char}}{m_{input} \times DM_{input}} \times 100\% \quad (1)$$

For the calculation of carbon yields, Equation (1) was supplemented by the carbon contents of DSS and HC and calculated as follows:

$$\text{Carbon yield } (\%_{db}) = \frac{m_{char} \times DM_{char} \times C_{char}}{m_{input} \times DM_{input} \times C_{input}} \times 100\% \quad (2)$$

Higher heating value (HHV) was calculated from the elemental analysis according to Channiwala and Parikh [30]:

$$\begin{aligned} &HHV\left(MJ\ kg_{db}^{-1}\right) = \\ &\quad 0.3491 \times C + 1.1783 \times H - 0.1005 \times S - 0.1034 \times O - 0.0051 \times N - 0.0211 \times Ash \end{aligned} \quad (3)$$

The calculated HHV from Equation (3) can be then used to determine the energy yield:

$$\text{Energy yield } (\%_{db}) = \frac{m_{char} \times DM_{char} \times HHV_{char}}{m_{input} \times DM_{input} \times HHV_{input}} \times 100\% \quad (4)$$

To determine the share of phosphorus in the liquid phase (P_{liquid}), the concentrations of phosphorus (c_P) in the DSS and HC are put into relation as follows:

$$P_{liquid}(\%) = \frac{m_{liquid} \times c_{P,liquid}}{m_{input} \times DM_{input} \times c_{P,input}} \times 100\% \quad (5)$$

2.5. Regression Modeling

Because the relationship between certain output variables from HTC reaction conditions was to be determined, a DoE/RSM approach was chosen to obtain the most information out of a limited number of experiments. Regression modelling was performed as described by Montgomery [31]. The FCCD was chosen to aim at fitting a second order model through the following equation:

$$\begin{aligned} y = \beta_0 + \beta_T x_T + \beta_t x_t + \beta_{pH} x_{pH} + \beta_{Tt} x_T x_t + \beta_{TpH} x_T x_{pH} + \beta_{tpH} x_t x_{pH} + \beta_{T^2} {x_T}^2 \\ + \beta_{t^2} {x_t}^2 + \beta_{pH^2} {x_{pH}}^2 + \varepsilon \end{aligned} \quad (6)$$

in which T denotes the reaction temperature, t the holding time after the reaction temperature was reached and pH the initial pH.

Equation (6) can also be expressed as:

$$y = X\beta + \varepsilon \quad (7)$$

where y is a vector of the measured responses (e.g., dry matter content), X is a matrix containing information about the levels of the variables at which the responses were obtained, β is the vector of regression coefficients, and ε is a vector of random errors. With the aim to find the values of the β's that minimize the sum of squares of ε, the least squares estimates are calculated by:

$$\hat{\beta} = (X'X)^{-1} X'y \quad (8)$$

The regression model can now be estimated as:

$$\hat{y} = X\,\hat{\beta} \quad (9)$$

and the difference between measured responses (y) and fitted values ($\hat{y}$) is given in the vector of residuals:

$$e = y - \hat{y} \quad (10)$$

Analysis of variance was used to refine the regression model by testing the significance of each of the terms in Equation (6) by conducting an *F*-test. The *F*-value of a term (e.g., temperature) was calculated by comparing the mean squares of the evaluated term (MS_{Term}) and the remaining residuals ($MS_{Residual}$):

$$F_0 = \frac{MS_{Term}}{MS_{Residual}} = \frac{SS_{Term}/df_{Term}}{SS_{Residual}/df_{Residual}} \quad (11)$$

with SS denoting the sum of squares and df the degrees of freedom. F_0 was tested against $F_{Stat}(\alpha, df_{Term}, df_{Residual})$ on a significance level of $\alpha = 0.1$ and if $F_0 > F_{stat}$, it was concluded that there are significant effects caused by the evaluated term. After the model was refined to include only statistically relevant terms, it was further improved by testing to exclude outliers (results from one or more experiments) from the model. For each term, a *t*-value was calculated for each run, according to Weisberg [32]:

$$t_i = \frac{\hat{e}_i}{MS_{Residual,i}\sqrt{1 + x_i'(X'_i X_i)^{-1} x_i}} \quad (12)$$

The designation i denotes that data from the ith run was excluded during the calculation and x is essentially a vector containing the first row of X. The *t*-value was compared with $t_{Stat}(\alpha/2, n - p - 1)$, where *n* denotes the total number of runs and *p* the number of parameters in the model. If $|t_i| < t_{Stat}$, the run was excluded from regression modelling.

To give the reader an impression of the regression model quality, the metrics predictive and adjusted R^2 are provided. R^2, the coefficient of determination, expresses how much variation around the mean is explained by the model and is calculated as follows:

$$R^2 = 1 - \frac{SS_{Residual}}{SS_{Model} + SS_{Residual}} \quad (13)$$

where SS_{Model} denotes the sum of squares of the model, which is calculated by adding up all SS_{Term} of the terms included in the model. If the model captures all variation around the mean, R^2 equals one, and if the model cannot account for any variation, R^2 equals zero. R^2 is closest to one when all terms are still in the model and can thus mislead to include terms in the model that do not contribute a statistically significant effect. An adjusted R^2 (R^2_{adj}) accounts for this and, therefore, decreases as the number of model terms increases if the additional terms do not improve the model. Additionally, predictive R^2 (R^2_{pred}) expresses the predictive ability of the model. It takes into account the variation that arises when excluding one run from the model and using it to predict this value [31].

Regression modeling and data plotting were performed with the software packages Design Expert 12 (Stat-Ease, Inc., Minneapolis, MN, USA) and Origin 2020 (OriginLab Corp., Northampton, MA, USA).

3. Results and Discussion

3.1. Regression Modeling

For the parameters of interest, dewaterability, and phosphorus release, as well as general HC characteristics energy, carbon, and solid yield, regression models were developed and are presented in Table 2. The calculation of the *F*-test (Equation (11)) indicated which model coefficients are statistically relevant, which means that they are adding more information than noise to the model. Factors that were not included in any model ($x_T \times x_t$ and $x_t \times x_{pH}$) were excluded from the table.

Table 2. Coded regression model coefficients for hydrochar (HC) and process water properties.

Target Value	Coded Regression Model Coefficients							Metrics	
	x_T	x_t	x_{pH}	$x_T \times x_{pH}$	${x_T}^2$	${x_t}^2$	${x_{pH}}^2$	R^2_{adj}	R^2_{pred}
Hydrochar Characteristics									
Dry matter (%)	2.70		−3.90	2.22	−1.87			0.89	0.84
Carbon content ($\%_{daf}$)	2.12	0.61	2.52	1.31		−0.90		0.92	0.90
HHV (MJ kg_{db}^{-1})	−0.23		−0.16		0.31			0.63	0.53
Solid yield ($\%_{db}$)	−3.36		5.19	−4.09				0.72	0.69
Carbon yield ($\%_{db}$)	−4.39		4.62	−3.40				0.72	0.69
Energy yield ($\%_{db}$)	−4.95		4.04	−4.01				0.78	0.74
Process Water Properties									
P content (mg L^{-1})	−159.55		−2260.21	163.81			1720.72	0.99	0.99
P share (%)	−2.56		−31.46	3.64			24.97	0.99	0.98
Final pH (-)	0.10	0.11	2.17		0.32		−0.87	0.99	0.99

daf = dry and ash-free basis; db = dry basis; P = phosphorus.

The displayed models were further refined by the exclusion of outliers by conducting a *t*-test (Equation (12)). Because of the experimental design (FCCD) and the repetitions of corner and central points, outliers could be excluded without having to limit the order of the model, which led to regression models with good predictive and adjusted R^2 in most cases. The coded regression model

coefficients indicate by how much the response is expected to change when the input parameter is changed by one unit. By default, the coded units range from −1 for the lowest level and +1 for the highest level. In this study, the change by one unit relates to a temperature change of 20 °C, holding time change of 30 min or a pH change of 3.1. The comparison of the coefficient's magnitude within a response allows for an estimation of the relative impact that each input parameter has.

Table 2 shows that reaction temperature and initial pH have a statistically significant (at least $p < 0.05$) influence on the output parameters in all models while holding time is only included in two models. As the absolute values of the coefficients of reaction temperature and initial pH are of similar magnitude for HC characteristics, it can be assumed that the effect of changing the temperature by 20 °C is similar to a pH change of 3.1. Even though holding time is included for carbon content, its value is the smallest, which relates to a small influence on the actual model. These trends are different for the investigated process water properties where pH has 12–21 times higher effects compared to temperature. In addition, the final pH is equally influenced by reaction temperature as by holding time. In comparison with other RSM publications, Álvarez-Murillo et al. [19] observed a similar effect of temperature on the solid yield of olive stone ($-5.56 \times x_T$ whereby a temperature change of one unit corresponds to 30 °C). Holding time was included in the model, because their tested maximum duration of 10 h yielded a statistically relevant effect. Mäkelä et al. [17] encountered a much stronger influence on the solid yield (daf) treating industrial mixed sludge from a pulp and paper mill ($-27 \times x_T$ whereas a temperature change of one unit corresponds to 40 °C). This can be attributed to the higher temperatures that were investigated (180–260 °C) and the exclusion of the observed high ash contents for the calculation of the solid yields. Hence, greater differences in yield can be observed. A more in depth analysis of the investigated output parameters is included in the following sections.

3.2. Holding Time vs. Reaction Time

Because holding time does not cover the whole timespan during which reactions take place, a more inclusive measure was used to investigate if this would cause time to become statistically relevant. The time during which temperature in the reactor exceeded 140 °C was chosen as Wang et al. [7] implicated that reactions start taking place between 130 and 150 °C. Reaction time will now be referred to by t_{140} in this study. It should be noted that this value only applies to sewage sludge and should be carefully chosen depending on the input material. Holding time and reaction time for each experiment can be found in Table A1 in Appendix A.

Regression modeling was carried out analogous to the procedure described in the previous sub-chapter. The output parameters for which reaction time is statistically relevant and, thus, included in the regression model are shown in Table 3. Carbon content is still mainly dependent on reaction temperature and initial pH, but the influence of time increased by using reaction time instead of holding time in the model. A comparison of contour plots is provided in Figure A1 in Appendix A and the use of reaction time shows the expected trend that with increasing reaction time and temperature, the carbon content increases. This becomes not that clear when holding time is used for the model. While the model for HHV does not include holding time, it does so with reaction time. The general trends that were described in the previous subsection remain as can be observed in the comparison in Figure A2 in Appendix A. For the final pH, reaction temperature is now excluded from the model, but the influence of time is still marginal, compared to initial pH as would be expected. Not much changes when comparing the contour plots in Figure A3 in Appendix A.

Table 3. Coded regression model coefficients for hydrochar (HC) and process water properties with t_{140} reaction time instead of holding time.

Target Value	Coded Regression Model Coefficients							Metrics	
	x_T	$x_{t,140}$	x_{pH}	$x_T{*}x_{pH}$	$x_{t140}{*}x_{pH}$	$x_T{}^2$	$x_{pH}{}^2$	R^2_{adj}	R^2_{pred}
Hydrochar characteristics									
Carbon content ($\%_{daf}$)	1.72	1.04	2.56	1.34		−0.93		0.91	0.89
HHV (MJ $kg_{db}{}^{-1}$)	−0.17	−0.15	−0.17		0.16		0.35	0.73	0.61
Process water properties									
Final pH (-)		0.24	2.17				−0.59	0.99	0.99

daf = dry and ash-free basis; db = dry basis.

The refined data analysis with reaction time instead of holding time did not yield significantly different results. This shows that for batch experiments, variation of holding time does not have a significant influence on most output parameters. It could be considered to be kept constant in future DoEs, unless parameters such as carbon content, HHV, and final pH are of major interest and holding or reaction time will be varied in a much wider range. However, holding time is clearly important when developing continuous processes as it will alter the size of the equipment for a certain targeted mass flow. This has to be addressed with corresponding equipment in lab-scale to allow for a smaller difference between holding time and time above a certain reaction temperature.

3.3. Hydrochar Properties

To verify the results and to form a basis for comparison, a van-Krevelen-diagram was created (Figure 2) and common HC properties such as solid, carbon, and energy yield were calculated (Table 4). For reasons of clarity and comprehensibility, only a selection of HCs as well as DSS is shown in these illustrations. The HCs produced at the mildest (160 °C, 30 min, pH 7) and harshest conditions (200 °C, 90 min, pH 2) are shown to illustrate the range of reaction severity. To estimate the individual effect of the different reaction parameters, each parameter was varied from the mildest to the harshest condition while the other two remained at the mildest.

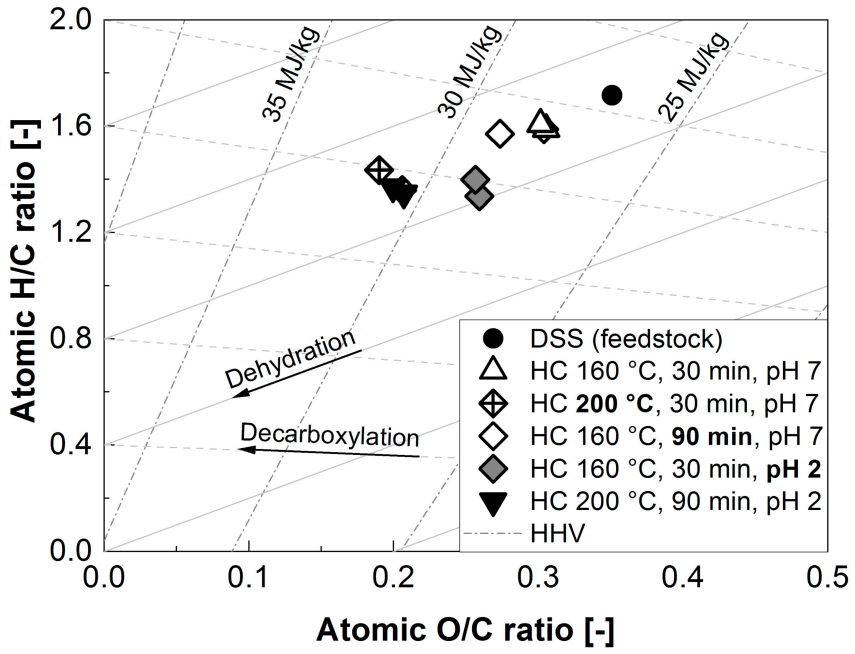


Figure 2. van-Krevelen-diagram of selected hydrochars (HC) and digested sewage sludge (DSS) at different process conditions.

Table 4. Hydrochar (HC) properties in relation to reaction conditions.

T (°C)	t (min)	pH (-)	C Content ($\%_{daf}$)	N Content ($\%_{daf}$)	HHV (MJ kg_{db}^{-1})	Solid Yield ($\%_{db}$)	C Yield ($\%_{db}$)	Energy Yield ($\%_{db}$)
160	30	7.5 ± 0.23	57.3 ± 0.04	4.6 ± 0.16	13.7 ± 0.27	90.0 ± 0.88	86.4 ± 2.02	92.1 ± 2.71
200	30	7.9 ± 0.23	63.8 ± 0.63	3.7 ± 0.19	13.0 ± 0.52	76.9 ± 0.69	71.9 ± 2.32	74.9 ± 3.68
160	90	7.7 ± 0.07	58.3 ± 1.02	4.4 ± 0.04	13.6 ± 0.00	85.8 ± 7.44	82.2 ± 6.94	87.5 ± 7.58
160	30	2.2 ± 0.14	55.5 ± 0.13	3.6 ± 0.09	14.5 ± 0.62	62.7 ± 18.60	62.4 ± 15.93	67.4 ± 17.24
200	90	2.1 ± 0.05	57.9 ± 0.45	3.1 ± 0.08	13.3 ± 0.07	74.2 ± 1.77	68.1 ± 1.46	73.5 ± 1.37

T = reaction temperature; t = holding time; C = carbon; N = nitrogen; HHV = higher heating value.

By visualizing the atomic H/C versus O/C ratios of DSS and HCs in Figure 2, insights into the governing reactions can be gained. Generally, carbonization decreases both H/C and O/C ratios and, depending on how the ratios change in relation, an assumption about the major governing reaction can be made. In this case, the atomic ratios of the HCs primarily follow dehydration, which confirms the finding of Wang and Li [33] that reactions at temperatures below 180 °C are governed by dehydration. When comparing the HCs that were both produced at 160 °C and pH 7, but at differing holding times of 30 and 90 min, it becomes apparent that varying the holding time between these time intervals does not have a noticeable effect. Contrarily, the variation of pH or temperature leads to a more severe conversion of the feedstock. The pH variation resulted in HCs with lower H/C ratios than caused by dehydration reactions only.

Considering the lower nitrogen contents of pH-adjusted HCs (Table 4), it seems like the pH adjustment favored deamination, which is besides decarboxylation the major conversion mechanism for proteins [22]. This causes the additional removal of hydrogen, resulting in a lower H/C ratio. When analyzing the influence of temperature variation, HC produced at 200 °C possesses almost the same atomic ratios as the HC produced at the harshest combined conditions (200 °C, 90 min, pH 2).

It can be seen from the data that the initial calculated HHV based on dry matter of DSS is slightly higher (13.4 MJ kg_{db}^{-1}, Table 1) than the HHV of some of the produced HCs (12.7–15.0 MJ kg_{db}^{-1}). This is due to the accumulation of ash in HC (increasing ash content from 40.9$\%_{db}$ in DSS to 39.2–53.4$\%_{db}$ in HC). Calculating HHV on a dry and ash free basis (daf) results in the expected increase when comparing the resulting chars (26.0–30.9 MJ kg_{daf}^{-1}) with the initial DSS (22.6 MJ kg_{daf}^{-1}). The HC characteristics solid, carbon, and energy yield were calculated according to the described approach (Equations (1), (2), and (4), respectively). They follow the expected trajectory that more severe reactions result in lower yields. Conducting an analysis of variance for the respective yields showed for reaction temperature ($p < 0.01$), initial pH ($p < 0.001$), and their interaction ($p < 0.05$) to have statistically significant effects on the yields. The regression models in terms of actual factors (T in °C, t in min and pH) are as follows:

$$\text{Solid yield } (\%_{db}) = 40.14 + 0.16x_T + 13.64x_{pH} - 0.066x_T \times x_{pH} \quad (14)$$

$$\text{Carbon yield } (\%_{db}) = 56.28 + 0.057x_T + 11.45x_{pH} - 0.055x_T \times x_{pH} \quad (15)$$

$$\text{Energy yield } (\%_{db}) = 59.31 + 0.079x_T + 13.04x_{pH} - 0.065x_T \times x_{pH} \quad (16)$$

In contrast to the majority of studies, holding time was found not to be statistically relevant in these experiments. This is because others investigated a much longer time span [18,19]. Therefore, it can be concluded that for solid, carbon, and energy yield, a variation of holding time between 30 and 90 min does not cause statistically different results, and the time could be minimized. Danso-Boateng et al. [34] developed a regression model for the solid yield of primary sewage sludge (SY = 118.49 − $0.26x_T$ − $0.04x_t$, actual factors, range of 140–200 °C and 15–240 min) and it compares quite well with Equation (14) when set at a neutral pH of 7 (SY = 135.62 − $0.30x_T$, actual factors). Though holding time is included, the main effect comes from temperature, as found in this study.

The regression model of the solid yield is displayed as a contour plot in Figure 3 as a representative for the other yields, as they follow the same trend. It shows that mild conditions (low reaction

temperature and neutral pH) lead to higher solid, carbon, and energy yields. While Mäkelä et al. [18] found no effect of the addition of acid on the yields when investigating industrial mixed sludge from a pulp and paper mill, these experiments show a clear effect. This is likely to occur because a wider range of pH with a more concentrated acid was tested. Unlike Reza et al. [35], who found that mass yield was more affected by reaction temperature than initial pH when converting wheat straw, the opposite is indicated here with pH having 1.5 times the effect compared to that of reaction temperature.

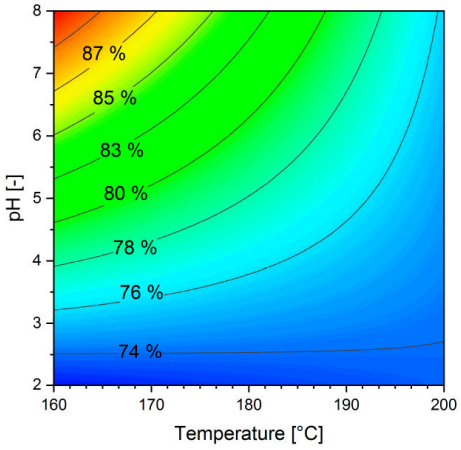


Figure 3. Regression model contour plot showing the influence of initial pH and reaction temperature on the solid yield ($\%_{db}$).

The dry matter content after mechanical dewatering was used as a measure of the increase in sludge dewaterability. Analysis of variance has shown that only the influence of reaction temperature ($p < 0.001$) and initial pH ($p < 0.001$) was statistically relevant (see Table 2). Furthermore, their interaction ($p < 0.001$) as well as the quadratic term of temperature ($p < 0.01$) are included in the model due to their high significance level, resulting in the following equation with actual factors:

$$\text{Dry matter content } (\%) = -91.48 + 1.64x_T - 7.74x_{pH} + 0.036x_T \times x_{pH} - 0.0047{x_T}^2 \quad (17)$$

The resulting response contour, plotted in Figure 4, shows the general trend that low pH and higher temperatures favor dewaterability. Initial pH has a clear and strong influence, as a more acidic initial pH yields increasing dry matter contents. A deviation from the expected trend exists at low pH levels, where an increase in reaction temperature does not result in ever increasing dry matter contents. This trend is caused by the quadratic term ${x_T}^2$ in the regression model, which causes the slight curvature. However, when determining to what extent this term contributes to the model by comparing the SS of the term ${x_T}^2$ to the total SS, it becomes clear that it contributes only with 5% to the model and should not be emphasized.

The regression model of the dry matter content is in agreement with Danso-Boateng et al. [8], Gao et al. [36], and Wang et al. [37], who also found a strong influence of temperature on dewaterability, but not of holding time. When the threshold time of 30 min is exceeded, there is no longer any holding time dependency according to Wang et al. [37]. At the selected temperatures, the typical HTC reactions already take place sufficiently and another increase in temperature will yield even faster reactions. Because dehydration and decarboxylation cause a decrease in hydrophilic functional groups, such as hydroxyl and carboxyl groups [38], the product is more easily dewatered already by a simple mechanical press. The effect of acidic pH on improved dewaterability can be explained by the enhancement of dehydration reactions, caused by sulfuric acid [39], which adds to the temperature effect. Dewaterability is additionally improved by the floc structure disintegration, which releases the bound water as free water [22]. Escala et al. [9], who conducted a comparable experiment, achieved similar dry matter contents. They were able to reach a dry matter content of 52 ± 5.5% after applying a

pressure of 40 bar to HC produced at 205 °C and 24 min. This is higher than the 45.6 ± 2.24% achieved in this study at comparable reaction conditions (200 °C, 30 min, pH 2 and 7) and is very likely due to a much lower dewatering pressure.

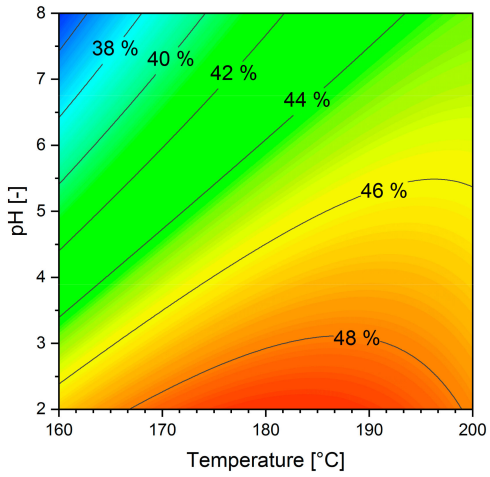


Figure 4. Regression model contour plot showing the influence of initial pH and reaction temperature on the dry matter content (%) after mechanical dewatering.

3.4. Phosphorus Release

For the phosphorus distribution, the pH value is the most significant driver and the variation of holding time showed no statistically relevant effect again, resulting in the following regression models with actual factors:

$$\text{Phosphorus content}\left(\text{mg L}^{-1}\right) = 12.97 - 0.021x_T - 3.03x_{pH} + 0.027x_T \times x_{pH} + 0.18{x_T}^2 \quad (18)$$

$$\text{Phosphorus share}\ (\%) = 204.32 - 0.42x_T - 47.22x_{pH} + 0.059x_T \times x_{pH} + 2.63{x_T}^2 \quad (19)$$

A lower initial pH generally leads to a lower pH value after the reaction (Figure 5a). This lower pH value favors the solution of phosphorus from the solid and the phosphorus concentration in the process water increases. The influence of the pH value is particularly evident in a range of the initial pH of 2–5 (Figure 5b).

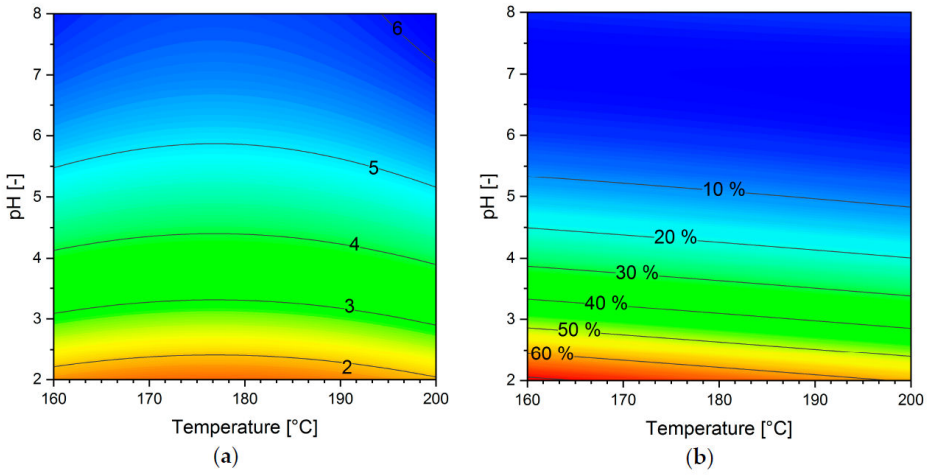


Figure 5. Regression model contour plots showing (**a**) the dependence of process water pH and (**b**) the dependence of liquid phase phosphorus release (% of total P) on reaction temperature and initial pH.

At neutral pH, not much phosphorus will be dissolved by varying holding time and reaction temperature. As others already found, most of the phosphorus is retained in the solid phase [9,13,22]. However, the variation of the initial pH has a major influence on the transfer of phosphorus into the liquid phase. When Shi et al. [14] reached an initial pH of 0.24 and applied HTC conditions of 170 °C and 30 min, they were able to transfer 83% of phosphorus into the liquid phase. The results of this study confirm their findings, as the maximum phosphorus share achieved in these experiments is 78% at 160 °C and an initial pH of 1.93. An even higher share of 88% was achieved in an experiment at 160 °C and an initial pH of 2.25 but was excluded as an outlier from the model as a result from the *t*-test according to Equation (12). It is, thus, possible to transfer phosphorus into the liquid phase to be potentially recovered by precipitation, e.g., as magnesium ammonium phosphate (struvite) [14], though this comes at the cost of high acid consumption. Additionally, precipitation of phosphorus in HTC process water brings additional challenges due to the huge variety of other components found in the process water.

The future upscaling of this process requires considerations regarding holding time, mixing behavior and heat transfer, especially because a continuous process is desired. While the results of this study show that the holding time can be minimized to 30 min for maximum dewaterability and phosphorus release in a batch process, this time needs to be assessed anew for the application in a continuous process. During the heating time in a batch process, the conversion of sewage sludge already begins and, therefore, the holding time of a batch cannot be directly transferred to a continuous process. More severe reaction conditions (higher reaction temperature and longer holding time) would be necessary, if energy densification and a further increase in HHV are desired [17].

4. Conclusions

The results of this study provide useful information for the design and optimization of HTC systems for sewage sludge treatment. It aimed at finding the optimal HTC reaction conditions for a maximized mechanical dewaterability and phosphorus release in the liquid phase. In the investigated design space (160–200 °C, 30–90 min, pH 1.93–8.09), low initial pH levels are desirable and holding time can be minimized as it had no statistically relevant effect. The influence of reaction temperature is not completely clear. While low temperatures are somewhat more advantageous for phosphorus release, medium temperatures are favorable for dewaterability.

It was investigated if using reaction time as an input parameter instead of holding time would cause different results. Though only minor changes were observed, some models were more refined. However, with regard to future experimental plans using batch reactors, aiming at identifying the impact of HTC process parameters on several product characteristics, it could be considered to exclude holding time from the parameter variation. Residence time is of course a main factor in the design of larger plants, but can only be addressed sufficiently in lab-scale using equipment allowing continuous operation to minimize actual heating and cooling times.

A numerical optimization to maximize mechanical dewaterability and phosphorus release yielded achievable dry matter contents of 48.6% and a phosphorus share of 70.3% in the liquid phase at 170 °C and an initial pH of 1.93. This would be accompanied by an HHV of 13.95 MJ kg_{db}^{-1}.

Author Contributions: Conceptualization, T.L. and B.W.; Formal analysis, T.L.; Funding acquisition, B.W.; Investigation, T.L.; Methodology, T.L. and B.W.; Project administration, T.L.; Supervision, B.W.; Validation, T.L. and B.W.; Visualization, T.L.; Writing—original draft, T.L.; Writing—review and editing, B.W. All authors have read and agreed to the published version of the manuscript.

Funding: This research received funding by the Federal Ministry of Food and Agriculture of Germany (BMEL) and by the Sächsische Aufbaubank (SAB) financed by the European Regional Development Fund (ERDF) under grant no. 100283030.

Acknowledgments: The authors would like to thank all of the laboratory and technical staff at DBFZ for conducting the experiments and analyses. Furthermore, the authors would like to thank L. Prokot for her contributions to the experimental part of this study.

Conflicts of Interest: The authors declare no conflict of interest.

Appendix A

Table A1. Experimental design (temperature, holding time, and pH) as well as reaction time and measured pH.

Experiment	T (°C)	T (min)	t_{140} (min)	pH, DoE (-)	pH, Measured (-)
1	160	90	275	7.0	7.8
2	180	60	251	4.5	5.6
3	200	90	411	7.0	8.1
4	160	30	130	2.0	2.1
5	160	90	274	7.0	7.7
6	200	30	247	2.0	2.3
7	160	30	144	7.0	7.7
8	200	30	207	7.0	7.8
9	200	90	365	7.0	7.1
10	160	30	147	7.0	7.4
11	180	60	221	7.0	7.3
12	180	30	178	4.5	5.3
13	160	90	274	2.0	2.2
14	200	30	236	2.0	2.2
15	180	60	264	2.0	2.1
16	160	90	280	2.0	1.9
17	180	90	352	4.5	5.5
18	200	60	324	4.5	5.5
19	160	60	194	4.5	5.3
20	200	90	398	2.0	2.1
21	180	60	251	4.5	5.4
22	180	60	272	4.5	5.4
23	180	60	241	4.5	5.4
24	160	30	155	2.0	2.3
25	200	30	242	7.0	8.1
26	200	90	413	2.0	2.0

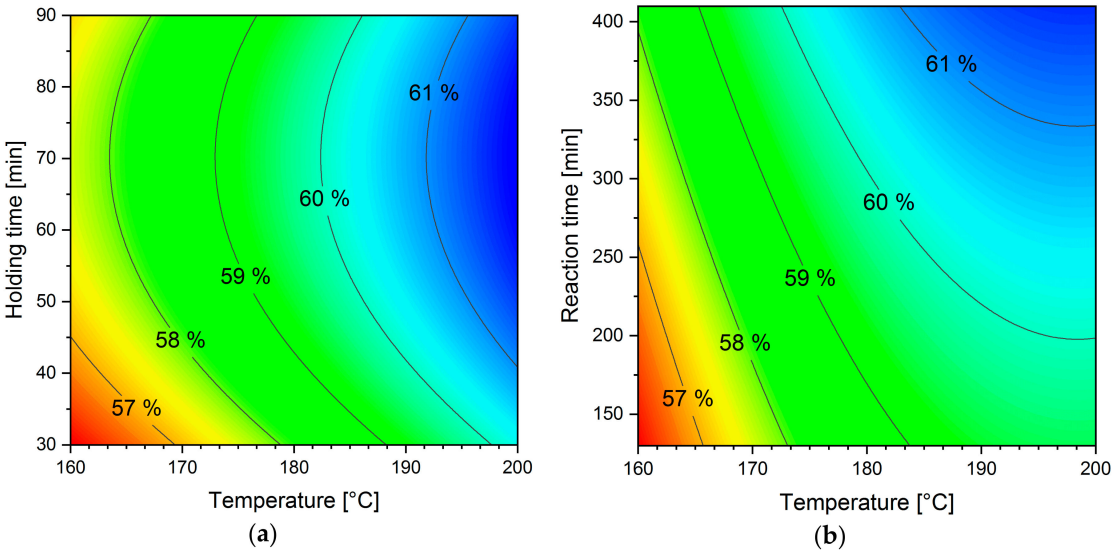


Figure A1. Regression model contour plots showing the dependence of carbon content ($\%_{daf}$) on reaction temperature and (**a**) holding time and (**b**) reaction time.

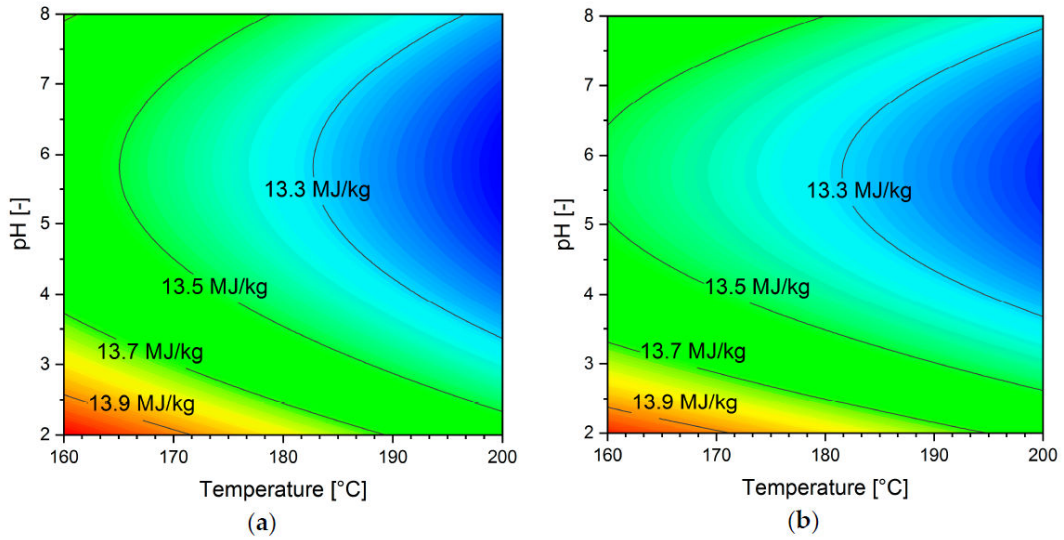


Figure A2. Regression model contour plots showing the dependence of the higher heating value (MJ kg_{TS}^{-1}) on reaction temperature and initial pH based on a model referring to (**a**) holding time and (**b**) reaction time (contours shown at the respective time at the corresponding center point).

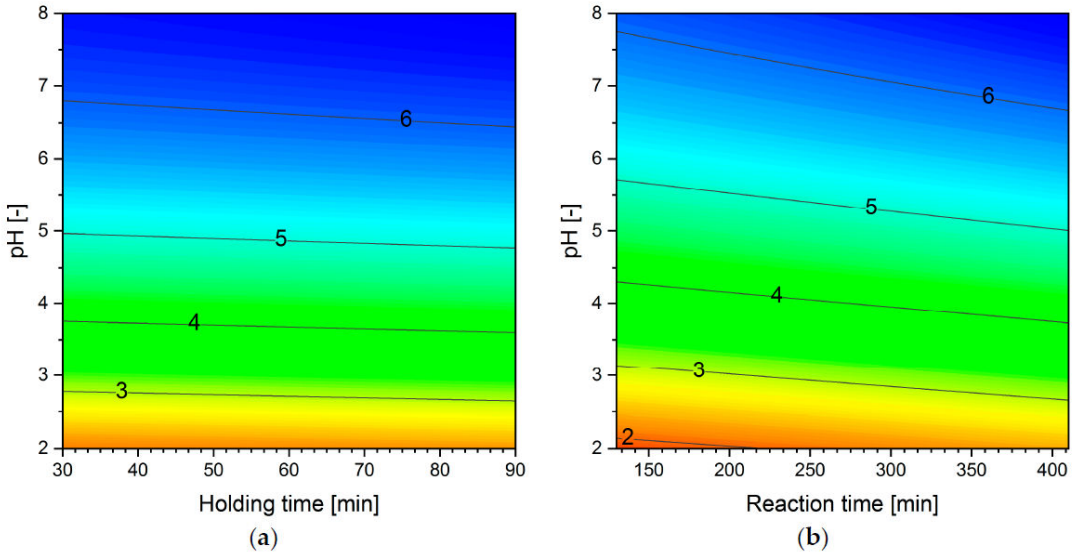


Figure A3. Regression model contour plots showing the dependence of the process water pH (-) on initial pH and (**a**) holding time and (**b**) reaction time.

References

1. Sterritt, R.M.; Lester, J.N. The value of sewage sludge to agriculture and effects of the agricultural use of sludges contaminated with toxic elements: A review. *Sci. Total Environ.* **1980**, *16*, 55–90. [CrossRef]
2. Beni, C.; Servadio, P.; Marconi, S.; Neri, U.; Aromolo, R.; Diana, G. Anaerobic Digestate Administration: Effect on Soil Physical and Mechanical Behavior. *Commun. Soil Sci. Plant Anal.* **2012**, *43*, 821–834. [CrossRef]
3. Hudcová, H.; Vymazal, J.; Rozkošný, M. Present restrictions of sewage sludge application in agriculture within the European Union. *Soil Water Res.* **2019**, *14*, 104–120. [CrossRef]
4. BMU. Verordnung über die Verwertung von Klärschlamm, Klärschlammgemisch und Klärschlammkompost-AbfKlärV. BGBl. I S. 3465. 2017. Available online: https://www.bmu.de/en/law/sewage-sludge-ordinance/ (accessed on 21 August 2020).
5. Raheem, A.; Sikarwar, V.S.; He, J.; Dastyar, W.; Dionysiou, D.D.; Wang, W.; Zhao, M. Opportunities and challenges in sustainable treatment and resource reuse of sewage sludge: A review. *Chem. Eng. J.* **2018**, *337*, 616–641. [CrossRef]

6. Werther, J.; Ogada, T. Sewage sludge combustion. *Prog. Energy Combust. Sci.* **1999**, *25*, 55–116. [CrossRef]
7. Wang, T.; Zhai, Y.; Zhu, Y.; Li, C.; Zeng, G. A review of the hydrothermal carbonization of biomass waste for hydrochar formation: Process conditions, fundamentals, and physicochemical properties. *Renew. Sust. Energ. Rev.* **2018**, *90*, 223–247. [CrossRef]
8. Danso-Boateng, E.; Holdich, R.G.; Wheatley, A.D.; Martin, S.J.; Shama, G. Hydrothermal carbonization of primary sewage sludge and synthetic faeces: Effect of reaction temperature and time on filterability. *Environ. Prog. Sustain. Energy* **2015**, *34*, 1279–1290. [CrossRef]
9. Escala, M.; Zumbühl, T.; Koller, C.; Junge, R.; Krebs, R. Hydrothermal Carbonization as an Energy-Efficient Alternative to Established Drying Technologies for Sewage Sludge: A Feasibility Study on a Laboratory Scale. *Energy Fuels* **2012**, *27*, 454–460. [CrossRef]
10. Meng, D.; Jiang, Z.; Yoshikawa, K.; Mu, H. The effect of operation parameters on the hydrothermal drying treatment. *Renew. Energy* **2012**, *42*, 90–94. [CrossRef]
11. Libra, J.; Ro, K.S.; Kammann, C.I.; Funke, A.; Berge, N.D.; Neubauer, Y.; Titirici, M.-M.; Fühner, C.; Bens, O.; Kern, J.; et al. Hydrothermal carbonization of biomass residuals: A comparative review of the chemistry, processes and applications of wet and dry pyrolysis. *Biofuels* **2011**, *2*, 71–106. [CrossRef]
12. Reza, M.T.; Andert, J.; Wirth, B.; Busch, D.; Pielert, J.; Lynam, J.G.; Mumme, J. Hydrothermal Carbonization of Biomass for Energy and Crop Production. *Appl. Bioenergy* **2014**, *1*, 11–29. [CrossRef]
13. Heilmann, S.M.; Molde, J.S.; Timler, J.G.; Wood, B.M.; Mikula, A.L.; Vozhdayev, G.V.; Colosky, E.C.; Spokas, K.A.; Valentas, K.J. Phosphorus reclamation through hydrothermal carbonization of animal manures. *Environ. Sci. Technol.* **2014**, *48*, 10323–10329. [CrossRef] [PubMed]
14. Shi, Y.; Luo, G.; Rao, Y.; Chen, H.; Zhang, S. Hydrothermal conversion of dewatered sewage sludge: Focusing on the transformation mechanism and recovery of phosphorus. *Chemosphere* **2019**, *228*, 619–628. [CrossRef]
15. Wang, T.; Zhai, Y.; Zhu, Y.; Peng, C.; Wang, T.; Xu, B.; Li, C.; Zeng, G. Feedwater pH affects phosphorus transformation during hydrothermal carbonization of sewage sludge. *Bioresour. Technol.* **2017**, *245*, 182–187. [CrossRef] [PubMed]
16. Ovsyannikova, E.; Arauzo, P.J.; Becker, G.C.; Kruse, A. Experimental and thermodynamic studies of phosphate behavior during the hydrothermal carbonization of sewage sludge. *Sci. Total Environ.* **2019**, *692*, 147–156. [CrossRef] [PubMed]
17. Mäkelä, M.; Benavente, V.; Fullana, A. Hydrothermal carbonization of lignocellulosic biomass: Effect of process conditions on hydrochar properties. *Appl. Energy* **2015**, *155*, 576–584. [CrossRef]
18. Mäkelä, M.; Benavente, V.; Fullana, A. Hydrothermal carbonization of industrial mixed sludge from a pulp and paper mill. *Bioresour. Technol.* **2016**, *200*, 444–450. [CrossRef]
19. Álvarez-Murillo, A.; Román, S.; Ledesma, B.; Sabio, E. Study of variables in energy densification of olive stone by hydrothermal carbonization. *J. Anal. Appl. Pyrolysis* **2015**, *113*, 307–314. [CrossRef]
20. Román, S.; Libra, J.; Berge, N.D.; Sabio, E.; Ro, K.S.; Li, L.; Ledesma, B.; Álvarez, A.; Bae, S. Hydrothermal Carbonization: Modeling, Final Properties Design and Applications: A Review. *Energies* **2018**, *11*, 216. [CrossRef]
21. Kieseler, S.; Neubauer, Y.; Zobel, N. Ultimate and Proximate Correlations for Estimating the Higher Heating Value of Hydrothermal Solids. *Energy Fuels* **2013**, *27*, 908–918. [CrossRef]
22. Wang, L.; Chang, Y.; Li, A. Hydrothermal carbonization for energy-efficient processing of sewage sludge: A review. *Renew. Sustain. Energ. Rev.* **2019**, *108*, 423–440. [CrossRef]
23. Deutsches Institut für Normung e. V. *Sludge, Treated Biowaste and Soil—Determination of pH (EN 15933:2012)*; German Version; Beuth Verlag GmbH: Berlin, Germany, 2012; DIN EN 15933:2012-11.
24. Deutsches Institut für Normung e. V. *Solid Biofuels—Sample Preparation (ISO 14780:2017)*; German Version; Beuth Verlag GmbH: Berlin, Germany, 2017; DIN EN ISO 14780:2017-08.
25. Deutsches Institut für Normung e. V. *Solid Biofuels—Determination of Moisture Content—Oven Dry Method—Part 3: Moisture in General Analysis Sample (ISO 18134-3:2015)*; German Version; Beuth Verlag GmbH: Berlin, Germany, 2015; DIN EN ISO 18134-3:2015-12.
26. Deutsches Institut für Normung e. V. *Solid biofuels—Determination of Total Content of Carbon, Hydrogen and Nitrogen—Instrumental Methods (EN 15104:2011)*; German Version; Beuth Verlag GmbH: Berlin, Germany, 2011; DIN EN 15104:2011-04.
27. Deutsches Institut für Normung e. V. *Solid Biofuels—Determination of Ash Content (EN 14775:2009)*; German Version; Verlag GmbH: Berlin, Germany, 2012; DIN EN 14775:2012-11.

28. Deutsches Institut für Normung e. V. *Solid Biofuels—Determination of Calorific Value (ISO 18125:2017)*; German Version; Verlag GmbH: Berlin, Germany, 2017; DIN EN ISO 18125:2017-08.
29. Deutsches Institut für Normung e. V. *Water quality—Determination of Selected Elements by Inductively Coupled Plasma Optical Emission Spectrometry (ICP-OES) (ISO 11885:2007)*; German Version; Beuth Verlag GmbH: Berlin, Germany, 2009; DIN EN ISO 11885:2009-09.
30. Channiwala, S.A.; Parikh, P.P. A unified correlation for estimating HHV of solid, liquid and gaseous fuels. *Fuel* **2002**, *81*, 1051–1063. [CrossRef]
31. Montgomery, D.C. *Design and Analysis of Experiments*, 8th ed.; John Wiley & Sons Inc.: Singapore, 2013; ISBN 978-1-118-09793-9.
32. Weisberg, S. *Applied Linear Regression*, 3rd ed.; Wiley-Interscience: Hoboken, NJ, USA, 2005; ISBN 9780471663799.
33. Wang, L.; Li, A. Hydrothermal treatment coupled with mechanical expression at increased temperature for excess sludge dewatering: The dewatering performance and the characteristics of products. *Water Res.* **2015**, *68*, 291–303. [CrossRef] [PubMed]
34. Danso-Boateng, E.; Shama, G.; Wheatley, A.D.; Martin, S.J.; Holdich, R.G. Hydrothermal carbonisation of sewage sludge: Effect of process conditions on product characteristics and methane production. *Bioresour. Technol.* **2015**, *177*, 318–327. [CrossRef]
35. Reza, M.T.; Rottler, E.; Herklotz, L.; Wirth, B. Hydrothermal carbonization (HTC) of wheat straw: Influence of feedwater pH prepared by acetic acid and potassium hydroxide. *Bioresour. Technol.* **2015**, *182*, 336–344. [CrossRef]
36. Gao, N.; Li, Z.; Quan, C.; Miscolczi, N.; Egedy, A. A new method combining hydrothermal carbonization and mechanical compression in-situ for sewage sludge dewatering: Bench-scale verification. *J. Anal. Appl. Pyrolysis* **2019**, *139*, 187–195. [CrossRef]
37. Wang, L.; Zhang, L.; Li, A. Hydrothermal treatment coupled with mechanical expression at increased temperature for excess sludge dewatering: Influence of operating conditions and the process energetics. *Water Res.* **2014**, *65*, 85–97. [CrossRef]
38. Funke, A.; Ziegler, F. Hydrothermal carbonization of biomass: A summary and discussion of chemical mechanisms for process engineering. *Biofuels Bioprod. Biorefining* **2010**, *4*, 160–177. [CrossRef]
39. Peterson, A.A.; Vogel, F.; Lachance, R.P.; Fröling, M.; Michael, J.; Antal, J.R.; Tester, J.W. Thermochemical biofuel production in hydrothermal media: A review of sub- and supercritical water technologies. *Energy Environ. Sci.* **2008**, *1*, 32–65. [CrossRef]



© 2020 by the authors. Licensee MDPI, Basel, Switzerland. This article is an open access article distributed under the terms and conditions of the Creative Commons Attribution (CC BY) license (http://creativecommons.org/licenses/by/4.0/).